Archives of Oral Biology 61 (2016) 115–124

Contents lists available at ScienceDirect

Archives of Oral Biology

journal homepage: www.elsevier.com/locate/aob

Intermittent hypoxia induces disturbances in craniofacial growth and defects in craniofacial morphology

Shuji Oishi[a], Yasuhiro Shimizu[a], Jun Hosomichi[a,*], Yoichiro Kuma[a], Hisashi Nagai[b], Hideyuki Maeda[b,d], Risa Usumi-Fujita[a], Sawa Kaneko[a], Chisa Shitano[a], Jun-ichi Suzuki[c], Ken-ichi Yoshida[b,d], Takashi Ono[a]

[a] Orthodontic Science, Department of Orofacial Development and Function, Division of Oral Health Sciences, Graduate School of Medical and Dental Sciences, Tokyo Medical and Dental University, 1-5-45 Yushima, Bunkyo-ku, Tokyo 113-8549, Japan
[b] Department of Forensic Medicine, Graduate School of Medicine, The University of Tokyo, 7-3-1 Hongo, Bunkyo-ku, Tokyo 113-0033, Japan
[c] Department of Advanced Clinical Science and Therapeutics, The University of Tokyo, 7-3-1 Hongo, Bunkyo-ku, Tokyo 113-0033, Japan
[d] Department of Forensic Medicine, Graduate School of Medicine, Tokyo Medical University, 6-1-1 Shinjuku, Shinjuku-ku, Tokyo 160-8402, Japan

ARTICLE INFO

Article history:
Received 15 July 2015
Received in revised form 2 October 2015
Accepted 19 October 2015

Keywords:
Intermittent hypoxia
Obstructive sleep apnea
Craniofacial growth
Bone mineral density
Growth retardation
Micro-CT analysis

ABSTRACT

Objectives: To investigate intermittent hypoxia (IH) induced changes in craniofacial morphology and bone mineral density (BMD) in the mandible of growing rats.
Design: Seven-week-old male Sprague-Dawley rats were exposed to IH for 4 days or 3 weeks. Sham-operated rats simultaneously breathed room air. Lateral and transverse cephalometric radiographs of the craniofacial region were obtained, and the linear distances between cephalometric landmarks were statistically analyzed. BMD and bone microstructure of the mandible were evaluated using micro-computed tomography (micro-CT).
Results: Cephalometric analyses demonstrated that exposure to IH only in the two groups for 3 weeks decreased the size of the mandibular and viscerocranial bones, but not that of the neurocranial bones, in early adolescent rats. These findings are consistent with upper airway narrowing and obstructive sleep apnea (OSA). Micro-CT showed that IH increased the BMD in the cancellous bone of the mandibular condyle and the inter-radicular alveolar bone in the mandibular first molar (M1) region.
Conclusions: This study is the first to identify growth retardation of the craniofacial bones in an animal model of sleep apnea. Notably, 3 weeks of IH can induce multiple changes in the bones around the upper airway in pubertal rats, which can enhance upper airway narrowing and the development of OSA. The reproducibility of these results supports the validity and usefulness of this model. These findings also emphasize the critical importance of morphometric evaluation of patients with OSA.

1. Introduction

Obstructive sleep apnea (OSA) is characterized by sleep-related collapse of the upper airway (Azagra-Calero, Espinar-Escalona, Barrera-Mora, Llamas-Carreras, & Solano-Reina, 2012). Understanding of the morbidity and pathophysiology of pediatric OSA has expanded significantly since the first report of this condition in 1976 (Guilleminault, Eldridge, Simmons, & Dement, 1976). However, the pathogenesis of pediatric OSA remains controversial because of the associated complications and age-related variations in presentation (Tan, Gozal, & Kheirandish-Gozal, 2013).

Risk factors for OSA in adults include hormonal imbalance (Barcelo et al., 2013), age (Mehra et al., 2007), sex (Bixler et al., 2001), diet (Papandreou et al., 2012), obesity (Azagra-Calero et al., 2012), and skeletal and soft tissue abnormalities (Aoki & Prahl-Andersen, 2007; Banno & Kryger, 2007). The severity and mortality of adult OSA are associated with various comorbidities (Azagra-Calero et al., 2012), such as heart failure, hypertension, arrhythmia, stroke, and diabetes mellitus. In contrast, pediatric OSA is often associated with impaired growth and development in the craniofacial and otolaryngological tissues, as well as with

Abbreviations: BMD, bone mineral density; IH, intermittent hypoxia; BV/TV, bone volume/tissue volume; M1 region, first molar region; micro-CT, micro-computed tomography; OSA, obstructives sleep apnea; ROI, region of interest.

* Corresponding author at: Orthodontic Science, Department of Orofacial Development and Function, Graduate School of Medical and Dental Sciences, Tokyo Medical and Dental University (TMDU), Tokyo, Japan. Tel.: +81 3 5803 5527; fax: +81 3 5803 5527.
E-mail address: hosomichi.orts@tmd.ac.jp (J. Hosomichi).

http://dx.doi.org/10.1016/j.archoralbio.2015.10.017
0003-9969/

neuromuscular diseases (Balbani, Weber, & Montovani, 2005; Huang & Guilleminault, 2012). Typically, children with OSA exhibit excessive daytime sleepiness, impaired school performance, abnormal daytime behavior, recent enuresis, morning headache, abnormal weight, and progressive development of hypertension (Azagra-Calero et al., 2012; Urschitz et al., 2003; Reade et al., 2004).

Children with OSA exhibit growth retardation in various ways (Ersoy, Yuceturk, Taneli, Urk, & Uyanik, 2005), including growth hormone deficiency, as well as snoring (Nieminen et al., 2002). Because skeletal and soft tissues in the nasopharyngeal and oropharyngeal regions undergo substantial development during puberty (Ronen, Malhotra, & Pillar, 2007), even mild impairment in craniofacial growth may cause a severe morphometric mismatch between the maxilla and the mandible. However, few studies have documented the possible association between craniofacial changes and the pathophysiology of OSA in puberty (Tapia et al., 2008; Yuan et al., 2012).

Adults with OSA show variable ventilatory responses to chemical stimulation (Radwan et al., 2000), whereas children with OSA exhibit ventilatory depression under anesthesia or in the presence of high carbon dioxide levels (Strauss, Lynn, Bratton, & Nespeca, 1999). Compared with adults, children present a greater reduction in oxygen saturation from the baseline to the nadir during sleep (Hara et al., 2013). This low oxygen saturation in children with OSA can result in general growth retardation (Poets, 1998) and weight loss (Martinez, Vasconcellos, de Oliveira, & Konrad, 2008). In children with moderate and severe OSA, the recurrent episodes of abnormal gas exchange during sleep cause hypoxemia, hypercapnia, and acidosis (Sharp, Druz, D'Souza, & Diamond, 1985).

A few reports have implicated impaired respiration in craniofacial development. For instance, a 3-day nasal obstruction in young rats has been shown to induce long-term hormonal changes that may result in craniofacial growth retardation (Padzys, Tankosic, Trabalon, & Martrette, 2012). Moreover, adult and elderly patients with OSA reportedly develop increased bone density (Uzkeser et al., 2013; Sforza, Thomas, Barthélémy, Collet, & Roche, 2013). Although intermittent hypoxia (IH) has been strongly implicated in the pathogenesis of OSA (Noda et al., 1998; Lal, Strange, & Bachman, 2012), the role of IH in the growth of the craniofacial bones of children with OSA has not been reported.

We recently developed an apparatus that enables simultaneous exposure of many rats to IH for long periods of time, thereby reproducibly simulating the pathogenesis of OSA (Maeda et al., 2013). Here, we implemented this approach to investigate the effect of IH on craniofacial development, bone mineral density (BMD), and bone microarchitecture in peripubertal rats during the stage of craniofacial growth modification.

2. Materials and methods

2.1. Experimental IH model

The experimental procedures were performed according to the Guide for the Care and Use of Laboratory Animals published by the US National Institutes of Health (NIH publication 85-23, revised 1996). The animal protocol was approved by the Institutional Animal Care and Use Committee of The University of Tokyo (approval number, P12-149).

Eighteen 7-week-old male Sprague-Dawley rats were used in this study. Experimental rats were exposed to IH at a rate of 20 cycles per hour (nadir, 4% oxygen; peak, 21% oxygen; 0% carbon dioxide), and control rats breathed room air. The control cage was placed next to the cage equipped with the IH apparatus, and all rats underwent their respective treatments for 8 h per day during the 12-hour "lights on" period (Maeda et al., 2013). The rats were randomly divided into 4 groups. The experimental rats underwent IH for 4 days (IH_{4D} group, $n=4$) or for 3 weeks (IH_{3W} group, $n=5$), while the control rats breathed room air for 4 days (C_{4D} group, $n=4$) or for 3 weeks (C_{3W} group, $n=5$). The experiments were conducted while the rats were 7–10 weeks of age, when craniofacial bones actively develop (puberty), as documented by studies of craniofacial growth (Spence, 1940) and puberty onset (Cheung, Thornton, Nurani, Clifton, & Steiner, 2001) in male rats. All rats were allowed free access to food and water throughout the experimental period, as previously described (Maeda et al., 2013; Skelly et al., 2012). After the IH-exposure period, all rats were anesthetized by a sodium pentobarbital injection and sacrificed.

2.2. Cephalometric analysis

To evaluate craniofacial growth, we obtained lateral and dorsoventral radiographs with a soft X-ray machine (SOFTEX CMB-2; SOFTEX Co., Ltd., Tokyo, Japan). The head position of each rat was fixed using a pair of ear rods to maintain a standard head posture and contact with the film in any other way to avoid the magnification factor (Abbassy, Watari, & Soma, 2008). The sagittal and transverse cephalometric radiograph settings were 50 kVp, 15 mA, and 5-s impulses. All radiographs were taken, developed, and scanned by the same operator. Thirteen lateral and six dorsoventral landmarks were identified on the cephalometric radiographs (Fig. 1,Table 1). Sixteen linear distances between the cephalometric landmarks (Table 2) were measured, as described in previous studies (Abbassy et al., 2008; da Silva & Cecanho, 2009). To ensure reliability and reproducibility of each measurement, each distance was measured thrice by the same operator and the three values were averaged. The ratios of different craniofacial linear distances to the neurocranium were calculated by the cranial

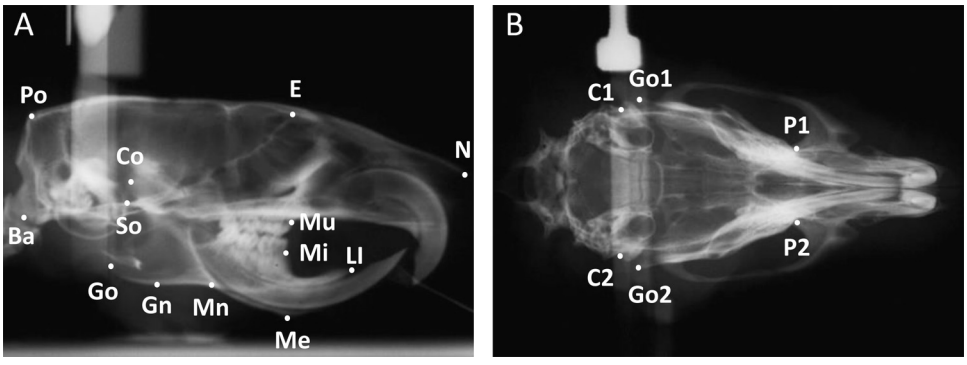

Fig. 1. Cephalometric landmarks. (A) Sagittal view. (B) Transverse view. Abbreviations: see Table 1.

Table 1
Definitions of cephalometric landmarks.

Sagittal cephalometric radiograph	
N	The most anterior point on the nasal bone
E	The intersection of the frontal bone and floor of anterior cranial fossa
Po	The most posterior and superior point on the skull
Ba	The most posterior and inferior point on the occipital condyle
So	The intersection of the most anterior tympanic bulla and the superior border of the sphenoid bone
Co	The most posterior and superior point on the mandibular condyle
Go	The most posterior point on the mandibular ramus
Mn	The most concave portion of the concavity on the inferior border of the mandibular corpus
Gn	The most inferior point on the ramus that lies on a perpendicular bisector of the line Go–Mn
Me	The most inferior and anterior point of the lower border of the mandible
LI	The most anterior and superior point on the alveolar bone of the mandibular incisor
Mi	The junction of the alveolar bone and the mesial surface of the first mandibular molar
Mu	The junction of the alveolar bone and the mesial surface of the first maxillary molar
Transverse cephalometric radiograph	
Go1, Go2	The points on the angle of the mandible that produce the widest width; Go1 is the point on the left side point and Go2 the point on the right
P1, P2	The most anterior and medial points within the temporal fossae that produce the most narrow palatal width; P1 is the point on the left and P2 is the point on the right
C1, C2	The points on the cranium that produce the widest cranial width; C1 is the point on the left and C2 is the point on the right

Table 2
Cephalometric measurements of the craniofacial skeleton.

Neurocranium	
Po–N	Total skull length
Po–E	Cranial vault length
Ba–E	Total cranial base length
So–E	Anterior cranial base length
Ba–So	Posterior cranial base length
Po–Ba	Posterior neurocranium height
Viscerocranium	
E–N	Nasal length
E–Mu	Viscerocranial height
Mandible	
Co–LI	Total mandibular length
Co–Me	Length from condylar head to Me
Co–Gn	Ramus height
Go–Mn	Posterior corpus length
Mi–LI	Anterior corpus length
Transverse measurements	
Go1–Go2	Bigonial width
C1–C2	Maximum cranial width
P1–P2	Palatal width

vault length (Po−E) to evaluate the discrepancies in craniofacial morphology. Additionally, The tibial length was radiographically measured from the proximal end to the medial malleolus of the tibia as an index for whole body growth.

2.3. Three-dimensional microcomputed tomography analysis

To investigate the changes in the bony microstructure of the condyles of the mandibular condyle and the inter-radicular alveolar bone in the mandibular first molar (M1) region, the cancellous bone was analyzed in both the IH_{3W} and C_{3W} groups using microcomputed tomography (micro-CT) with a desktop X-ray micro-CT system (SMX-100CT; Shimadzu, Kyoto, Japan). The region of interest (ROI) for structural morphometry was chosen within the cancellous bone of the mandibular condyle and the mandibular M1 region according to previous studies (Fig. 2) (Shimizu, Hosomichi, Kaneko, Shibutani, & Ono, 2011; Kuroda et al., 2011; Abbassy, Watari, & Soma, 2010). The mandibular condyle in the IH_{3W} and C_{3W} groups was analyzed to evaluate the influence of IH on the skeletal development of the mandible in rats. The ROI ($1.0 \times 1.0 \times 0.2$ mm) was selected in a region 1.0 mm distant from the epiphyseal cartilage of the mandibular condyle, to distinguish the ROI from the cortical bone area (Fig. 2A) (Kuroda et al., 2011; Bouxsein et al., 2010). The inter-radicular alveolar bone in the mandibular M1 region used for micro-CT was measured in the ROI for structural morphometry, as this area is frequently used for histomorphometry of the trabecular bone. The ROI was selected between the alveolar ridge crest and apex of the roots in the sagittal section. The white part showed the ROI between the four roots in the mandibular M1 region on the horizontal section. (Fig. 2B) (Shimizu et al., 2011; Abbassy et al., 2010). Each mandibular condyle and mandibular M1 region was analyzed with respect to the BMD, bone volume/tissue volume (BV/TV), trabecular bone thickness (Tb.Th), and trabecular number using a three-dimensional image-analysis software (TRI/3D-BON; Ratoc System Engineering, Tokyo, Japan) as follows. A scanning resolution of 20 μm was used to assess the mandibular condyle and alveolar bone in the M1 region (Shimizu et al., 2011; Kuroda et al., 2011; Abbassy et al., 2010). A CT-level histogram of the bone marrow was constructed to determine the adaptive threshold using the discriminant analysis method (Bouxsein et al., 2010).

2.4. Statistical analysis

Statistical calculations were performed using a statistical analysis software (IBM SPSS Statistics Version 20.0, Chicago, IL, USA). The control and experimental groups were compared using the Mann–Whitney *U*-test, and statistical significance was accepted at a p level of less than 0.05.

3. Results

3.1. Systemic changes in rats after IH

The body weight and tibial length of the rats were measured as an index for whole body growth. After 3 weeks of IH exposure, the body weight of rats exposed to IH was significantly lower than those of control rats (Fig. 3A). There was no significant difference in the tibial length between C_{3W} and IH_{3W} rats (Fig. 3B). The correlation between the body weight and tibia length was assessed by the Pearson correlation coefficient, which indicated a lower value ($p = 0.054$). This showed that the correlation between the body weight and whole body growth in this model was low.

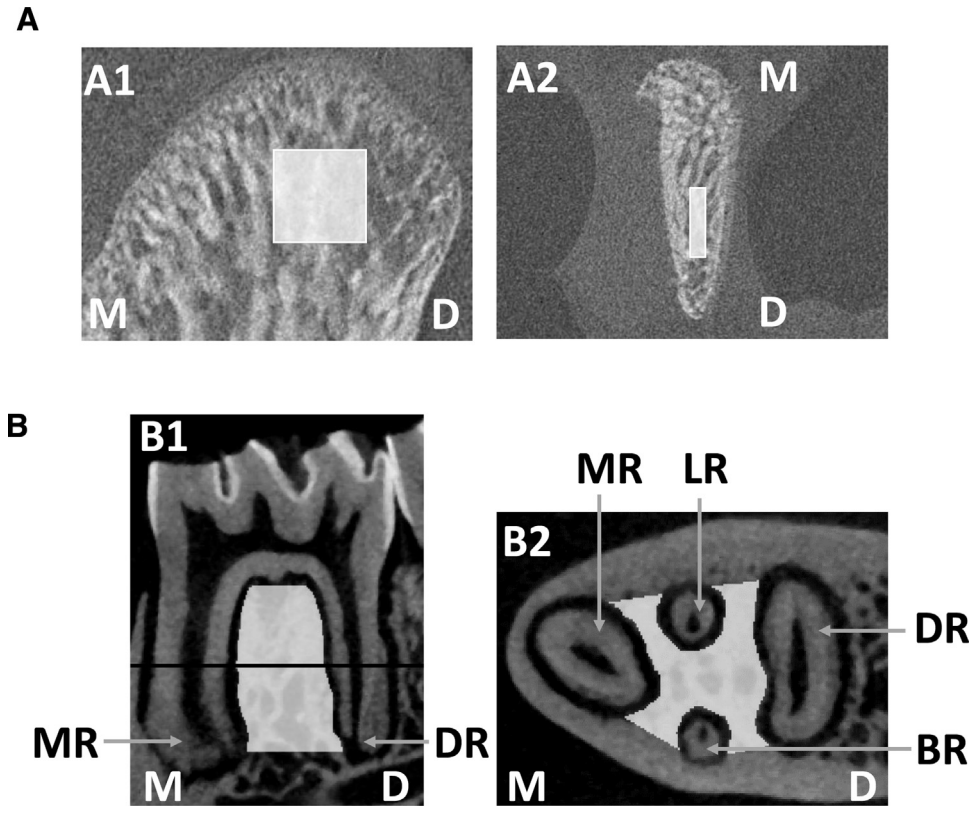

Fig. 2. Micro-CT images of the cancellous bone in the mandibular condyle and the inter-radicular alveolar bone in the mandibular first molar. (A) The region of interest (ROI; white-filled area) in the cancellous bone of condyle was selected in the sagittal section (A1) and in horizontal section (A2). (B) The region of interest (ROI; white-filled area) in the mandibular first molar region was selected in the sagittal section (B1) and in horizontal section (B2). Abbreviations: M, mesial; D, distal; MR, mesial root; BR, buccal root; DR, distal root; LR, lingual root.

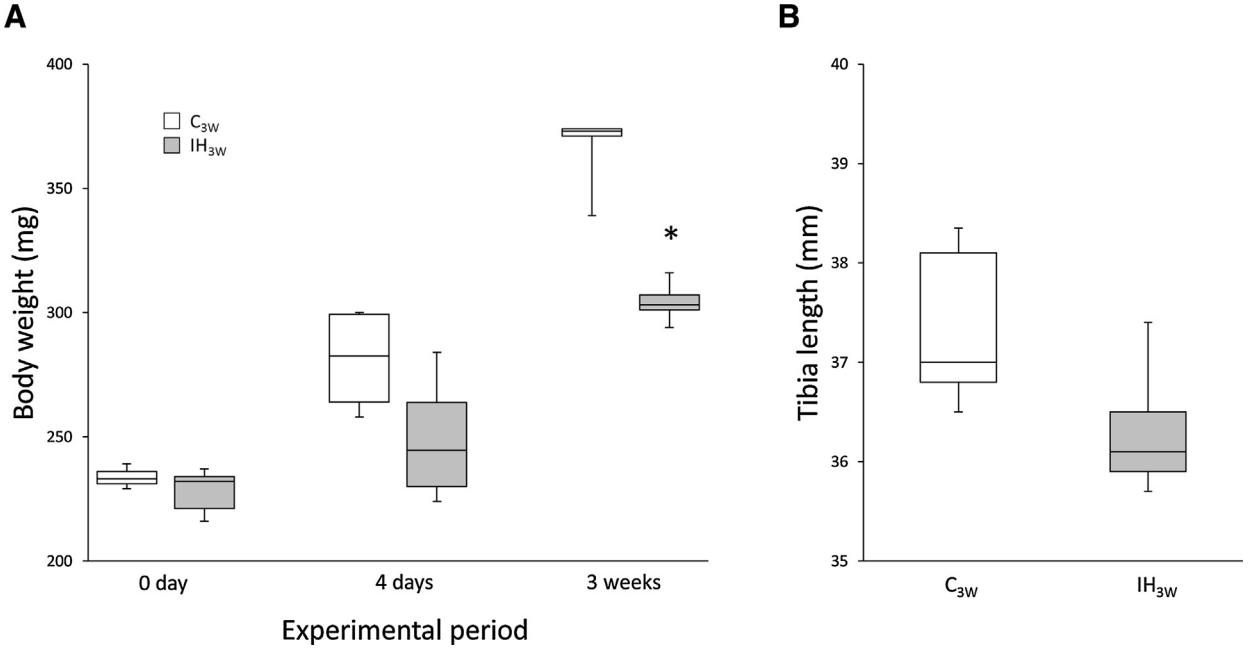

Fig. 3. Body weight and length of the tibia. (A) Body weight of the rats. (B) Length of the tibia after 3 weeks of intermittent hypoxia (IH). C, control group; IH, experimental group. $^{*}p < 0.05$.

3.2. Cephalometric measurements

No significant differences in any linear measurements were observed between the IH_{4D} and C_{4D} groups (Table 3). However, several parameters were significantly different between the IH_{3W} and C_{3W} groups. Among the 16 parameters examined, 5 parameters were found to be significantly different between the IH_{3W} and C_{3W} groups. In the viscerocranial measurements, the length of the nasal

Table 3
Comparison of skeletal cephalometric measurements between the C_{4D} and IH_{4D} groups and between the C_{3W} and IH_{3W} groups.

Group	C_{4D}		IH_{4D}		Significance	C_{3W}		IH_{3W}		Significance
Parameter	Medians	Standard errors	Medians	Standard errors		Medians	Standard errors	Medians	Standard errors	
Neurocranium										
Po–N	47.75	0.34	48.2	0.35	NS	50.6	0.29	49.5	0.22	NS
Po–E	28.85	0.39	29.4	0.32	NS	28.8	0.18	29.4	0.22	NS
Ba–E	30.85	0.30	31.85	0.21	NS	32.4	0.12	32.4	0.22	NS
So–E	20.00	0.33	20.65	0.06	NS	20.8	0.14	21	0.19	NS
Ba–So	12.15	0.18	12.15	0.05	NS	12.1	0.16	11.8	0.07	NS
Po–Ba	10.75	0.09	10.8	0.05	NS	11.0	0.15	11	0.12	NS
Viscerocranium										
E–N	19.85	0.28	19.2	0.35	NS	21.8	0.19	20.8	0.21	*
E–Mu	11.85	0.11	11.9	0.15	NS	13.3	0.28	12.2	0.09	NS
Mandible										
Co–LI	25.35	0.52	26.55	0.24	NS	27.9	0.22	27.4	0.20	*
Co–Me	21.9	0.17	22.05	0.05	NS	25.6	0.30	24.0	0.32	*
Co–Gn	11.05	0.16	10.9	0.25	NS	12.8	0.10	12.6	0.12	NS
Go–Mn	13.35	0.74	12.55	0.52	NS	14.5	0.26	12.5	0.54	*
Mi–LI	7.1	0.05	7.0	0.24	NS	7.70	0.20	8.0	0.24	NS
Transverse X-ray										
Go1–Go2	18.85	0.07	18.95	0.14	NS	19.4	0.11	18.7	0.14	*
C1–C2	17.35	0.09	17.25	0.07	NS	17.2	0.08	16.9	0.06	NS
P1–P2	6.95	0.13	6.65	0.21	NS	7.9	0.17	7.60	0.09	NS

Abbreviations: NS, nonsignificant; others, see Fig. 1 and Table 2.
* $p < 0.05$.

bone (E–N) was significantly shorter in IH_{3W} rats than in C_{3W} rats. Among the mandibular measurements, the total mandibular length (Co–L1), the length from the condylar head to the most inferior and anterior points of the lower border of the mandible

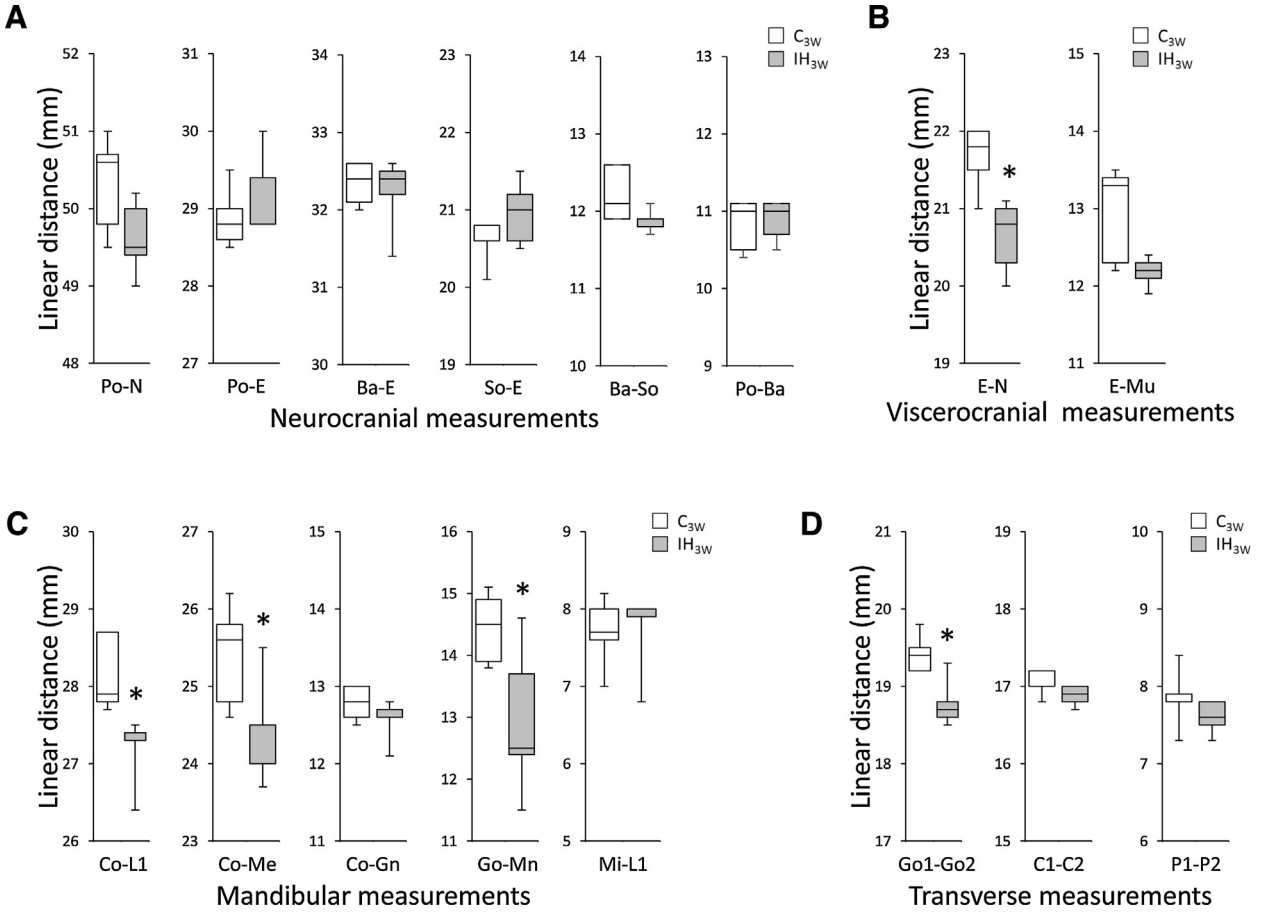

Fig. 4. Comparison of craniofacial measurements between the C_{3W} and IH_{3W} groups. Values of the (A) neurocranial, (B) viscerocranial, (C) mandibular, and (D) transverse measurements normalized. Data are shown as medians with standard errors for each group. Abbreviations: see Fig. 1 and Table 2. *$p < 0.05$.

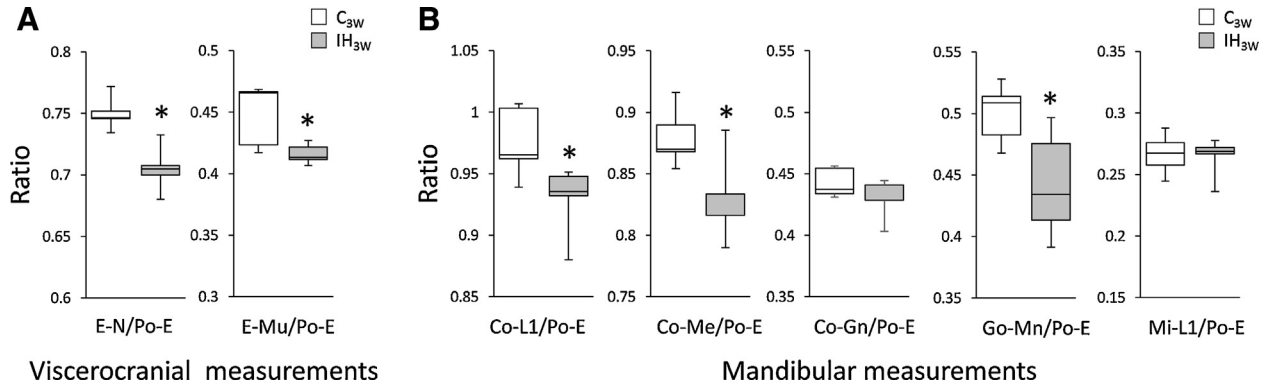

Fig. 5. Evaluation of craniofacial bony length ratios. The ratios of the (A) viscerocranial and (B) mandibular lengths to the cranial vault length (Po–E) were compared between the C_{3W} and IH_{3W} groups. Data are shown as medians with standard errors for each group. Abbreviations: see Fig. 1 and Table 2. $^{*}p < 0.05$.

(Co–Me), and the posterior corpus length (Go–Mn) were significantly shorter in IH_{3W} rats than in C_{3W} rats. Among neurocranial measurements, there was no difference in the total skull length or any other measurement between the C_{3W} and IH_{3W} groups. However, the bigonial width (Go1–Go2) was significantly lower in the IH_{3W} group than in the C_{3W} group (Fig. 4, Table 3).

3.3. Evaluation of craniofacial bony length ratios

Both the ratio of the viscerocranial length to the neurocranium length and the ratio of the mandibular length to the neurocranium length were significantly shorter in IH_{3W} rats than in C_{3W} rats. There was no significant difference in other ratios between the IH and control groups (Fig. 5).

3.4. Three-dimensional microcomputed tomography analysis

Micro-CT images of the cancellous bone in the mandibular condyle and the inter-radicular alveolar bone in the mandibular M1 region showed higher bone volume density for the cancellous bone in the IH_{3W} group than in the C_{3W} group (Figs. 6 and 7). As shown in Fig. 8, a micro-CT analysis demonstrated significantly higher BMD and BV/TV of the mandibular condyle and the mandibular M1 region in the IH_{3W} group than in the C_{3W} group.

4. Discussion

Here, for the first time, we have revealed evidence of heterogeneous growth retardation in the craniofacial bones in an animal model exposed to IH. These morphological changes can contribute to upper airway obstruction.

The purpose of our study was to provide evidence for the multifactorial pathogenesis of OSA and advocate early OSA treatment in children on the basis of bone and respiratory physiology. IH reportedly encompasses the primary aspects of OSA (Fletcher, 2001). However, given the multiple factors that contribute to the pathogenesis of OSA, such as hypercapnia, intrathoracic negative pressure, sympathetic overactivation, and

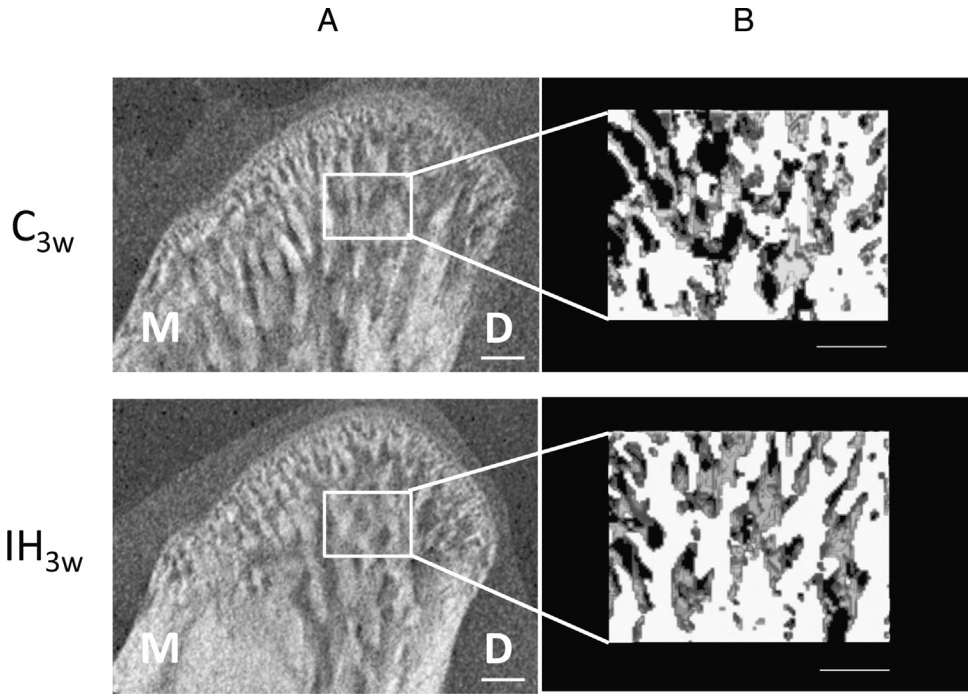

Fig. 6. Microarchitecture of the cancellous bone in the mandibular condyle of the rats in the C_{3W} and IH_{3W} groups. (A) Three-dimensional microcomputed tomography (micro-CT) morphology of the mandibular condyle in the sagittal section. The region of interest (ROI) was selected only in the cancellous bone, without the cortical bone. (B) Representative micro-CT images of the cancellous bone in the mandibular condyle. Scale bar: 500 μm. Abbreviations: M, mesial; D, distal.

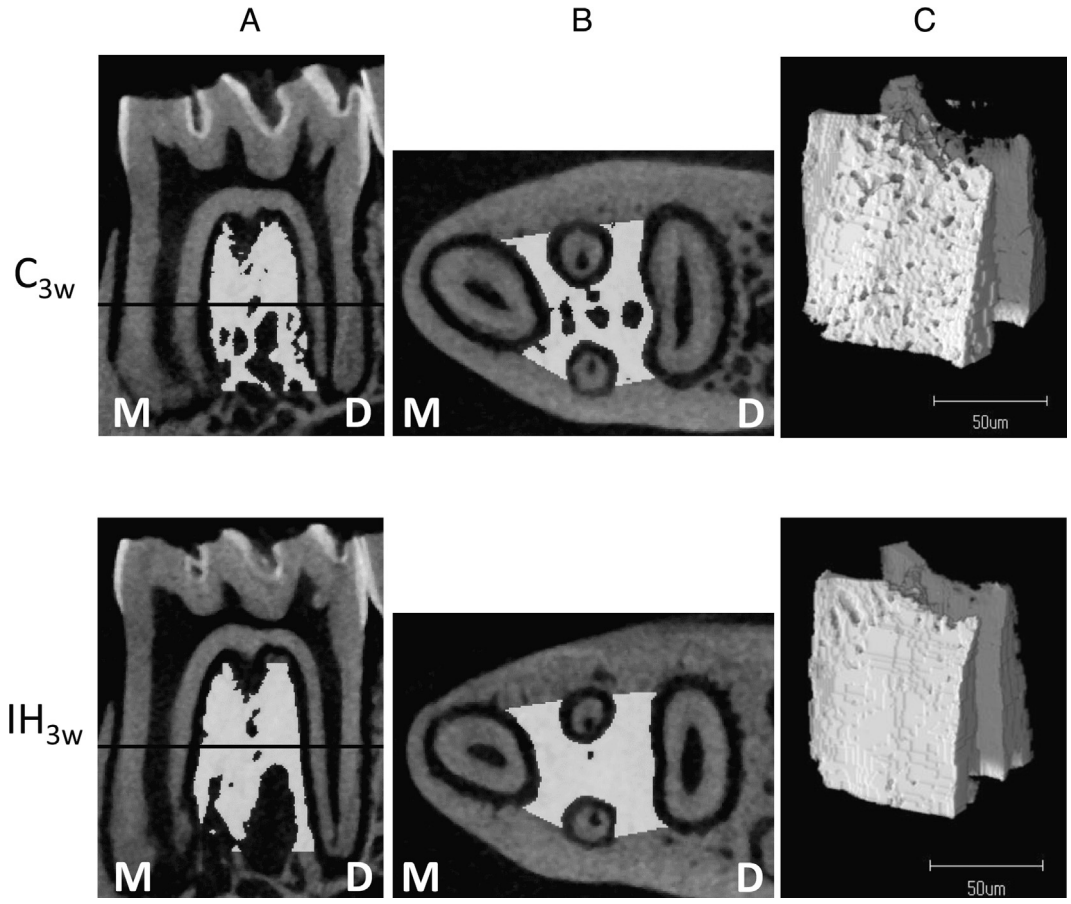

Fig. 7. Microarchitecture of the inter-radicular alveolar bone in the mandibular first molar region of the rats in the C_{3W} and IH_{3W} groups. Three-dimensional microcomputed tomography (micro-CT) morphology of the inter-radicular alveolar bone (indicated as white-filled area) in the mandibular first molar region in the sagittal section (A) and horizontal section (B). (C) Representative micro-CT images of alveolar bone in the mandibular first molar. Scale bar: 50 μm. Abbreviations: M, mesial; D, distal.

neurohumoral factors (Fletcher, 2001), it was surprising that 3 weeks of IH can induce significant morphological changes in the craniofacial bones consistent with OSA (Kuma et al., 2014). The horizontal lengths of the mandible and viscerocranium of IH_{3W} rats were shorter than those of C_{3W} rats, whereas the neurocranial lengths did not differ between the two groups. The latter changes can reduce the upper airway width and aggravate the pathogenesis of OSA.

We studied the effect of IH on growing rats aged from 7 to 10 weeks. During this stage of rat development, the mandibular and viscerocranial bones, but not the neurocranial bones, are in an active growth phase (Spence, 1940). The directional growth of craniofacial bones is affected by orofacial functional changes, such as respiratory obstruction (Padzys et al., 2012). Experimental hypoxia causes the inhibition of postsynaptic components in the rat vestibular nuclei (Yoshida, Sasa, & Takaori, 1988), which are connected with the spinal trigeminal nuclei, which, in turn, mediate the pathway of the jaw-opening reflex (Pinganaud, Bourcier, Buisseret-Delmas, & Buisseret, 1999; Tolu et al., 1996). Upper airway obstruction, which induces hypoxia in the rat (Trabalon & Schaal, 2012), affects the jaw-opening reflex and reduces the masticatory efficiency (Funaki, Hiranuma, Shibata, Kokai, & Ono, 2014). Orofacial functional demands under impaired inhalation may further influence the differential effects of IH on the skeletal growth among various craniofacial regions.

Given the lack of morphometric analysis in previous studies, such studies in rats exposed to IH are critical for elucidating the pathogenesis and treatment of OSA. Partly because of the high reproducibility of our experimental design, the morphological changes were significant despite the short duration of IH (3 weeks). Our findings strengthen the validity and usefulness of this rat IH model in research into the pathogenesis of OSA, particularly during early puberty.

The results of this study suggest that IH induces bony changes that can disturb airflow in the upper airway, further precipitating the development of OSA. Adenotonsillectomy has been widely and successfully adopted in children to alleviate upper airway stenosis (Marcus et al., 2012). The growth retardation of the craniofacial bones in rats exposed to IH suggests that IH evoked by adenotonsil hypertrophy induces bony growth retardation, thereby aggravating upper airway narrowing and OSA development. Clinical studies should investigate whether adenotonsillectomy can improve craniofacial growth retardation and OSA symptoms (such as snoring and the apnea–hypopnea index), in order to elucidate the causal link between impaired airflow (IH) and craniofacial growth retardation of adolescents with OSA.

The results of cephalometric measurements suggested that the mandibular measurements in the IH3W group were significantly smaller than those in the C3W group. However, there were no significant differences in neurocranium measurements between the IH_{3W} and C_{3W} groups (Fig. 4). These results suggest that the effect of IH on neurocranium bone growth is lower than that on the mandible, which induced disturbances in bone growth and density in rat maxillofacial bone (Fig. 5). Some of the most compelling previous studies on the effect of IH-related factors on osteogenesis have indicated that the mechanisms responsible for intramembranous ossification differ from those that cause endochondral ossification (Wang et al., 2007). This suggests that IH can increase

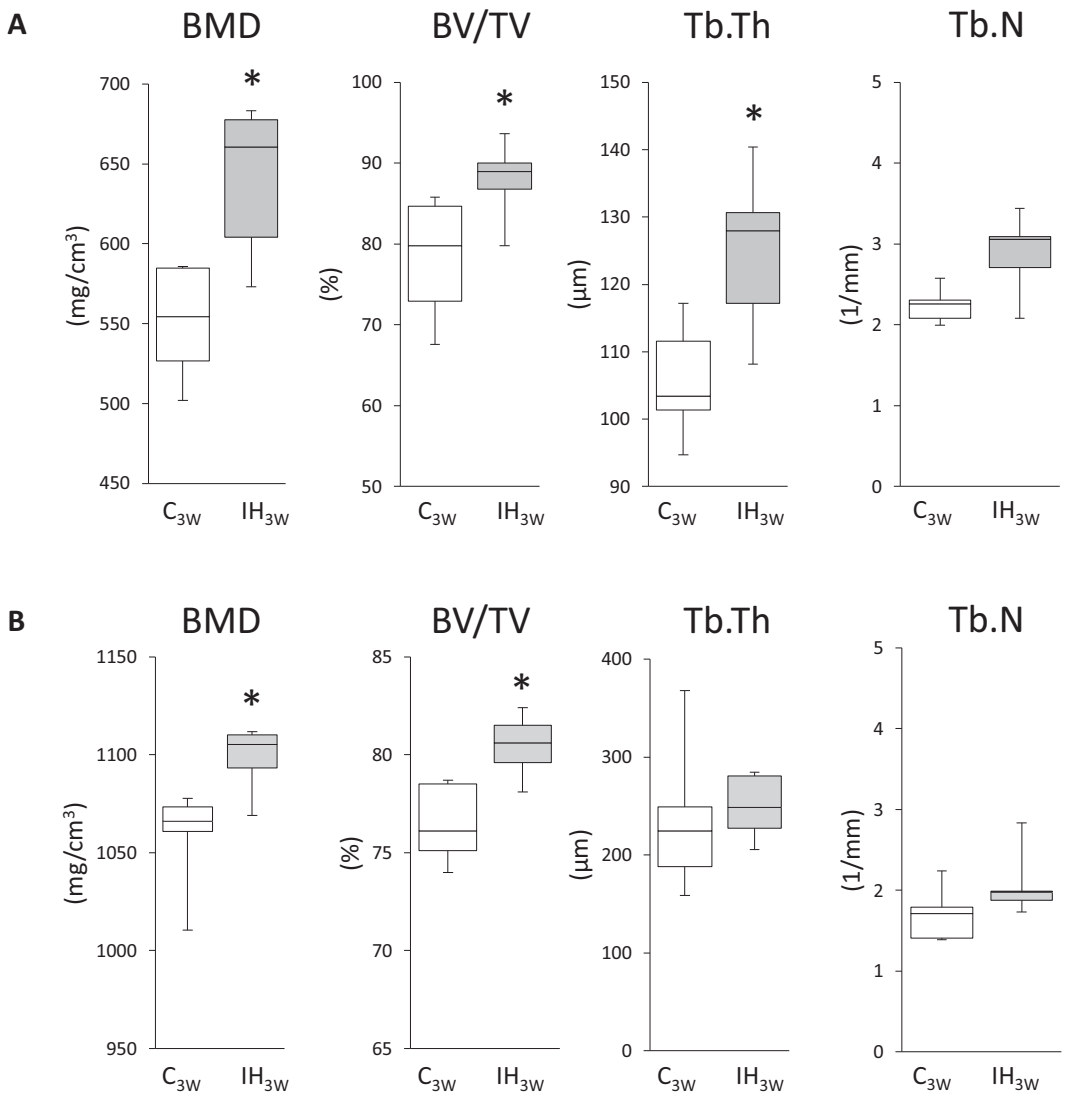

Fig. 8. Comparisons of bone morphology between the C_{3W} and IH_{3W} groups by microcomputed tomography analysis. The cancellous bone of the mandibular condyle (A) and the inter-radicular alveolar bone in the mandibular first molar region (B) were compared between the C_{3W} and IH_{3W} groups. Abbreviations: BMD, bone mineral density; BV/TV, bone volume/tissue volume; Tb.Th, trabecular bone thickness; Tb.N, trabecular number. Data are shown as medians with standards errors for each group. $^{*}p < 0.05$.

bone-modeling events in the growing long bone. Our results are consistent with the concept that IH affects the growth of the long bones, such as the mandible.

Osteogenesis is a complex process consisting of several steps (Chatakun et al., 2014). We speculated that IH may have differential effects on skeletal elongation and bone mineralization. Thus, we also investigated the BMD in the cancellous bone of the mandibular condyle and the inter-radicular alveolar bone in the mandibular M1 region to evaluate the effects of IH on mandibular bone mineralization. Indeed, there have been 2 discrepant clinical reports on the BMD in patients with OSA: the first one found an association with low density and osteoporosis in middle-aged patients (Uzkeser et al., 2013) and the other found an association with high density in elderly patients (Sforza et al., 2013). A previous study in an animal model, using old-aged mice exposed to chronic IH, suggested that IH did not modify BMD (Torres et al., 2013), and the spinal bone density was shown to be enhanced in old-aged rats that underwent 5 weeks of IH (Guner et al., 2013). In contrast to these reports, our study of growing rats indicated that IH significantly increased BMD as a potential risk factor for disturbances in craniofacial growth and discrepancies in craniofacial morphology. In our study, exposure to IH for 3 weeks enhanced BMD in the rat mandible. To date, no study has reported on bone metabolism in children and young adults with OSA. The clinical implications of the enhanced bone density in the mandible remain to be addressed. Therefore, the findings of current clinical studies remain inconclusive with respect to the relationship between OSA and bone metabolism according to the patients' age.

Changes in the bony microstructure during growth may have been associated with retardation of condylar growth in IH-exposed rats in this study, although further histomorphological studies would be necessary to verify the state of bone turnover and its relationship with the three-dimensional trabecular microstructure.

5. Conclusions

This is the first report on growth retardation in the craniofacial bones of pubertal rats that had been exposed to IH. Our study indicated that IH can affect rat maxillofacial bone growth, leading to aberrant maxillofacial morphology in the peripubertal growth period. These changes can enhance upper airway flow narrowing

and support the development of OSA. Thus, our model is both valid and useful. Moreover, we showed that IH induces changes in the bony microstructure of the mandible. Therefore, this study also emphasizes the importance of morphometric studies in patients with OSA.

Conflicts of interest

The authors declare that no competing interests exist.

Funding

Grant-in-Aid for Scientific Research (KAKENHI).

Ethical approval

The animal protocol was approved by the Institutional Animal Care and Use Committee of The University of Tokyo (approval number, P12-149).

Acknowledgment

This study was financially supported in part by Grants-in-Aid for Scientific Research (23593020, 23792420) from the Japanese Ministry of Education, Culture, Sports, Science and Technology.

References

Abbassy, M. A., Watari, I., & Soma, K. (2008). Effect of experimental diabetes on craniofacial growth in rats. *Archives of Oral Biology*, *53*(9), 819–825.
Abbassy, M. A., Watari, I., & Soma, K. (2010). The effect of diabetes mellitus on rat mandibular bone formation and microarchitecture. *European Journal of Oral Sciences*, *118*(4), 364–369.
Aoki, A., & Prahl-Andersen, B. (2007). Mandibular distraction osteogenesis for treatment of extreme mandibular hypoplasia. *American Journal of Orthodontics and Dentofacial Orthopedics*, *132*(6), 848–855.
Azagra-Calero, E., Espinar-Escalona, E., Barrera-Mora, J. M., Llamas-Carreras, J. M., & Solano-Reina, E. (2012). Obstructive sleep apnea syndrome (OSAS). Review of the literature. *Medicina Oral, Patología Oral y Cirugía Bucal*, *17*(6), e925–e929.
Balbani, A. P., Weber, S. A., & Montovani, J. C. (2005). Update in obstructive sleep apnea syndrome in children. *Brazilian Journal of Otorhinolaryngology*, *71*(1), 74–80.
Banno, K., & Kryger, M. H. (2007). Sleep apnea: clinical investigations in humans. *Sleep Medicine*, *8*(4), 400–426.
Barcelo, A., Esquinas, C., Pierola, J., De la Pena, M., Sanchez-de-la-Torre, M., Montserrat, J. M., et al. (2013). Vitamin D status and parathyroid hormone levels in patients with obstructive sleep apnea. *Respiration*, *86*(4), 295–301.
Bixler, E. O., Vgontzas, A. N., Lin, H. M., Ten Have, T., Rein, J., Vela-Bueno, A., et al. (2001). Prevalence of sleep-disordered breathing in women: effects of gender. *American Journal of Respiratory and Critical Care Medicine*, *163*(Pt 1 (3)), 608–613.
Bouxsein, M. L., Boyd, S. K., Christiansen, B. A., Guldberg, R. E., Jepsen, K. J., & Muller, R. (2010). Guidelines for assessment of bone microstructure in rodents using micro-computed tomography. *Journal of Bone and Mineral Research*, *25*(7), 1468–1486.
Chatakun, P., Núñez-Toldrà, R., Díaz López, E. J., Gil-Recio, C., Martínez-Sarrà, E., Hernandez-Alfaro, F., et al. (2014). The effect of five proteins on stem cells used for osteoblast differentiation and proliferation: a current review of the literature. *Cellular and Molecular Life Sciences*, *71*(1), 113–142.
Cheung, C. C., Thornton, J. E., Nurani, S. D., Clifton, D. K., & Steiner, R. A. (2001). A reassessment of leptin's role in triggering the onset of puberty in the rat and mouse. *Neuroendocrinology*, *74*(1), 12–21.
da Silva, H. C., & Cecanho, R. (2009). Cephalometric changes produced by locally applied anabolic steroid in Wistar rats. *Archives of Oral Biology*, *54*(4), 389–395.
Ersoy, B., Yuceturk, A. V., Taneli, F., Urk, V., & Uyanik, B. S. (2005). Changes in growth pattern, body composition and biochemical markers of growth after adenotonsillectomy in prepubertal children. *International Journal of Pediatric Otorhinolaryngology*, *69*(9), 1175–1181.
Fletcher, E. C. (2001). Invited review: physiological consequences of intermittent hypoxia: systemic blood pressure. *Journal of Applied Physiology (1985)*, *90*(4), 1600–1605.
Funaki, Y., Hiranuma, M., Shibata, M., Kokai, S., & Ono, T. (2014). Effects of nasal obstruction on maturation of the jaw-opening reflex in growing rats. *Archives of Oral Biology*, *59*(5), 530–538.
Guilleminault, C., Eldridge, F. L., Simmons, F. B., & Dement, W. C. (1976). Sleep apnea in eight children. *Pediatrics*, *58*(1), 23–30.
Guner, I., Uzun, D. D., Yaman, M. O., Genc, H., Gelisgen, R., Korkmaz, G. G., et al. (2013). The effect of chronic long-term intermittent hypobaric hypoxia on bone mineral density in rats: role of nitric oxide. *Biological Trace Element Research*, *154*(2), 262–267.
Hara, Y., Noda, A., Miyata, S., Otake, H., Yasuda, Y., Okuda, M., et al. (2013). Comparison of oxygen desaturation patterns in children and adults with sleep-disordered breathing. *American Journal of Otolaryngology*, *34*(5), 537–540.
Huang, Y. S., & Guilleminault, C. (2012). Pediatric obstructive sleep apnea and the critical role of oral-facial growth: evidences. *Frontiers in Neurology*, *3*(184) .
Kuma, Y., Usumi-Fujita, R., Hosomichi, J., Oishi, S., Maeda, H., Nagai, H., et al. (2014). Impairment of nasal airway under intermittent hypoxia during growth period in rats. *Archives of Oral Biology*, *59*(11), 1139–1145.
Kuroda, Y., Yonemitsu, I., Hosomichi, J., Watari, I., Takei, M., Ishida, Y., et al. (2011). Intermittent posterior displacement of the rat mandible in the growth period affects the condylar cancellous bone. *The Angle Orthodontist*, *81*(6), 975–982.
Lal, C., Strange, C., & Bachman, D. (2012). Neurocognitive impairment in obstructive sleep apnea. *Chest*, *141*(6), 1601–1610.
Maeda, H., Nagai, H., Takemura, G., Shintani-Ishida, K., Komatsu, M., Ogura, S., et al. (2013). Intermittent-hypoxia induced autophagy attenuates contractile dysfunction and myocardial injury in rat heart. *Biochimica et Biophysica Acta*, *1832*(8), 1159–1166.
Marcus, C. L., Brooks, L. J., Draper, K. A., Gozal, D., Halbower, A. C., Jones, J., et al. (2012). Diagnosis and management of childhood obstructive sleep apnea syndrome. *Pediatrics*, *130*(3), e714–e755.
Martinez, D., Vasconcellos, L. F., de Oliveira, P. G., & Konrad, S. P. (2008). Weight loss and brown adipose tissue reduction in rat model of sleep apnea. *Lipids in Health and Disease*, *7*, 26.
Mehra, R., Stone, K. L., Blackwell, T., Ancoli Israel, S., Dam, T. T., Stefanick, M. L., et al. (2007). Prevalence and correlates of sleep-disordered breathing in older men: osteoporotic fractures in men sleep study. *Journal of the American Geriatrics Society*, *55*(9), 1356–1364.
Nieminen, P., Lopponen, T., Tolonen, U., Lanning, P., Knip, M., & Lopponen, H. (2002). Growth and biochemical markers of growth in children with snoring and obstructive sleep apnea. *Pediatrics*, *109*(4), e55.
Noda, A., Ito, R., Okada, T., Yasuma, F., Nakashima, N., & Yokota, M. (1998). Twenty-four-hour ambulatory oxygen desaturation and electrocardiographic recording in obstructive sleep apnea syndrome. *Clinical Cardiology*, *21*(7), 506–510.
Padzys, G. S., Tankosic, C., Trabalon, M., & Martrette, J. M. (2012). Craniofacial development and physiological state after early oral breathing in rats. *European Journal of Oral Sciences*, *120*(1), 21–28.
Papandreou, C., Schiza, S. E., Bouloukaki, I., Hatzis, C. M., Kafatos, A. G., Siafakas, N. M., et al. (2012). Effect of Mediterranean diet versus prudent diet combined with physical activity on OSAS: a randomised trial. *European Respiratory Journal*, *39*(6), 1398–1404.
Pinganaud, G., Bourcier, F., Buisseret-Delmas, C., & Buisseret, P. (1999). Primary trigeminal afferents to the vestibular nuclei in the rat: existence of a collateral projection to the vestibulo-cerebellum. *Neuroscience Letters*, *264*(1–3), 133–136.
Poets, C. F. (1998). When do infants need additional inspired oxygen? A review of the current literature. *Pediatric Pulmonology*, *26*(6), 424–428.
Radwan, L., Maszczyk, Z., Koziej, M., Franczuk, M., Koziorowski, A., Kowalski, J., et al. (2000). Respiratory responses to chemical stimulation in patients with obstructive sleep apnoea. *Monaldi Archives for Chest Disease*, *55*(2), 96–100.
Reade, E. P., Whaley, C., Lin, J. J., McKenney, D. W., Lee, D., & Perkin, R. (2004). Hypopnea in pediatric patients with obesity hypertension. *Pediatric Nephrology*, *19*(9), 1014–1020.
Ronen, O., Malhotra, A., & Pillar, G. (2007). Influence of gender and age on upper-airway length during development. *Pediatrics*, *120*(4), e1028–e1034.
Sforza, E., Thomas, T., Barthélémy, J. C., Collet, P., & Roche, F. (2013). Obstructive sleep apnea is associated with preserved bone mineral density in healthy elderly subjects. *Sleep*, *36*(10), 1509–1515.
Sharp, J. T., Druz, W. S., D'Souza, V., & Diamond, E. (1985). Effect of metabolic acidosis upon sleep apnea. *Chest*, *87*(5), 619–624.
Shimizu, Y., Hosomichi, J., Kaneko, S., Shibutani, N., & Ono, T. (2011). Effect of sympathetic nervous activity on alveolar bone loss induced by occlusal hypofunction in rats. *Archives of Oral Biology*, *56*(11), 1404–1411.
Skelly, J. R., Edge, D., Shortt, C. M., Jones, J. F., Bradford, A., & O'Halloran, K. D. (2012). Respiratory control and sternohyoid muscle structure and function in aged male rats: decreased susceptibility to chronic intermittent hypoxia. *Respiratory Physiology & Neurobiology*, *180*(2-3), 175–182.
Spence, J. M. (1940). Method of studying the skull development of the living rat by serial cephalometric roentgenograms. *The Angle Orthodontist*, *10*(3), 127–139.
Strauss, S. G., Lynn, A. M., Bratton, S. L., & Nespeca, M. K. (1999). Ventilatory response to CO_2 in children with obstructive sleep apnea from adenotonsillar hypertrophy. *Anesthesia & Analgesia*, *89*(2), 328–332.
Tan, H. L., Gozal, D., & Kheirandish-Gozal, L. (2013). Obstructive sleep apnea in children: a critical update. *Nature and Science of Sleep*, *5*, 109–123.
Tapia, I. E., Karamessinis, L., Bandla, P., Huang, J., Kelly, A., Pepe, M., et al. (2008). Polysomnographic values in children undergoing puberty: pediatric vs:adult respiratory rules in adolescents. *Sleep*, *31*(12), 1737–1744.
Tolu, E., Caria, M. A., Chessa, G., Melis, F., Simula, M. E., Podda, M. V., et al. (1996). Trigeminal motoneuron responses to vestibular stimulation in the guinea pig. *Archives Italiennes de Biologie*, *134*(2), 141–151.
Torres, M., Montserrat, J. M., Pavía, J., Dalmases, M., Ros, D., Fernandez, Y., et al. (2013). Chronic intermittent hypoxia preserves bone density in a mouse model of sleep apnea. *Respiratory Physiology & Neurobiology*, *189*(3), 646–648.
Trabalon, M., & Schaal, B. (2012). It takes a mouth to eat and a nose to breathe: abnormal oral respiration affects neonates' oral competence and systemic adaptation. *International Journal of Pediatrics*, *2012*, 207605.

Urschitz, M. S., Guenther, A., Eggebrecht, E., Wolff, J., Urschitz-Duprat, P. M., Schlaud, M., et al. (2003). Snoring, intermittent hypoxia and academic performance in primary school children. *American Journal of Respiratory and Critical Care Medicine*, *168*(4), 464–468.

Uzkeser, H., Yildirim, K., Aktan, B., Karatay, S., Kaynar, H., Araz, O., et al. (2013). Bone mineral density in patients with obstructive sleep apnea syndrome. *Sleep and Breathing*, *17*(1), 339–342.

Wang, Y., Wan, C., Deng, L., Liu, X., Cao, X., Gilbert, S. R., et al. (2007). The hypoxia-inducible factor alpha pathway couples angiogenesis to osteogenesis during skeletal development. *Journal of Clinical Investigation*, *117*(6), 1616–1626.

Yoshida, S., Sasa, M., & Takaori, S. (1988). Different sensitivity to hypoxia in neuronal activities of lateral vestibular and spinal trigeminal nuclei. *Stroke*, *19*(3), 357–364.

Yuan, H., Pinto, S. J., Huang, J., McDonough, J. M., Ward, M. B., Lee, Y. N., et al. (2012). Ventilatory responses to hypercapnia during wakefulness and sleep in obese adolescents with and without obstructive sleep apnea syndrome. *Sleep*, *35*(9), 1257–1267.